ORNL-5324

Thermal Aging Effects on the Mechanical Properties of Annealed 2¼ Cr-1 Mo Steel

R. L. Klueh

OAK RIDGE NATIONAL LABORATORY
OPERATED BY UNION CARBIDE CORPORATION · FOR THE DEPARTMENT OF ENERGY

Printed in the United States of America. Available from
the Department of Energy,
Technical Information Center
P.O. Box 62, Oak Ridge, Tennessee 37830
Price: Printed Copy $4.50; Microfiche $3.00

ORNL-5324
Distribution
Category
~~UC-79b, h, k~~

Contract No. W-7405-eng-26

METALS AND CERAMICS DIVISION

THERMAL AGING EFFECTS ON THE MECHANICAL PROPERTIES OF ANNEALED 2 1/4 Cr-1 Mo STEEL

R. L. Klueh

Date Published: November 1977

OAK RIDGE NATIONAL LABORATORY
Oak Ridge, Tennessee 37830
operated by
UNION CARBIDE CORPORATION
for the
DEPARTMENT OF ENERGY

CONTENTS

THERMAL AGING EFFECTS ON THE MECHANICAL PROPERTIES OF ANNEALED 2 1/4 Cr-1 Mo STEEL*

R. L. Klueh

ABSTRACT

Four commercially annealed tubing heats of 2 1/4 Cr-1 Mo steel were aged at 454, 510, and 566°C for various times up to 20,000 hr. Tensile tests were made at room temperature and at the aging temperature on specimens from each heat for each aging condition. Creep tests were made on specimens from two of the heats. Thermal aging significantly changed both the room temperature and the aging temperature tensile properties, the effect being greatest for tests at the aging temperature. The amount and magnitude of the strength changes varied from one heat to another. After aging for 20,000 hr at 454 and 510°C, the strength of one heat increased. However, the other three heats showed decreases in yield strength and ultimate tensile strength of up to 40%, the maximum effect occurring at 566°C. Similar large changes in creep-rupture properties were also observed.

The strength properties did not change continuously between 0 and 20,000 hr. Plots of yield strength and ultimate tensile strength against aging time contain local maxima and minima occurring at different times for the different heats. We concluded that strength changes were determined by the proeutectoid ferrite that makes up the bulk of the microstructure. For short aging times, molybdenum and carbon atoms or atom clusters in solution interact with dislocations to strengthen the steel by a process termed "interaction solid solution hardening." This process can lead to a maximum in the strength-aging time curve. As molybdenum and carbon are removed from solution by the formation of Mo_2C, dispersion hardening by this precipitate becomes the dominant strenghtening mechanism. After an optimum precipitate density, which leads to a strength maximum, Mo_2C coarsens, causing a strength decrease. In addition to Mo_2C coarsening, the steel is further weakened when the fine Mo_2C precipitate particles are replaced by large globular particles of eta-carbide.

---

*Work performed under ERDA/RDD 189a No. OH028, Steam Generator Materials.

INTRODUCTION

Because of its good strength, formability, weldability, and corrosion resistance, 2 1/4 Cr-1 Mo steel is widely used by the power and petroleum industries for the fabrication of pressure vessels. In the nuclear industry, the steel has been considered for use in sodium-heated steam generators that would operate in conjunction with liquid metal fast breeder reactors (LMFBRs). It is for this latter application that the work discussed in this report was carried out.

Since the initial carbides that form during heat treatment are unstable, 2 1/4 Cr-1 Mo steel undergoes metallurgical changes during elevated-temperature exposure. The precipitation reactions that occur have been studied,[1—3] but few studies have been made of their effect on mechanical properties. Recently, a limited amount of mechanical properties data became available[4] on steam piping that had been in service for up to 120,000 hr at 566°C. Creep-rupture and tensile properties were also determined[5] on 2 1/4 Cr-1 Mo steel specimens that were aged in helium and decarburized in sodium for 26,500 hr at 566°C. However, there do not appear to be any studies of the change in properties with aging time and at temperatures of interest for LMFBR steam generators (the upper operating temperature is about 510°C).

In the present work, four commercial tubing heats of the type used in conventional steam generators were aged to 20,000 hr at 454, 510, and 566°C. Tensile studies were made along with a limited number of creep-rupture tests.

EXPERIMENTAL

Four commercial air-melted tubing heats that were commercially annealed were obtained from Babcock and Wilcox Corporation (Table 1). This commercial "anneal" heat treatment is sometimes referred to as an "isothermal anneal" because the tubes are cooled from the austenitizing temperature to a temperature in the range from 677 to 732°C (where the transformation to proeutectoid ferrite occurs), held at this temperature for a given time, then cooled to room temperature. For tubes, the

Table 1. Chemical Composition of 2 1/4 Cr-1 Mo Steel Tubing Heats as Reported by Vendors

Heat	Chemical Composition, wt %						
	C	Mn	S	P	Si	Cr	Mo
36202	0.12	0.47	0.021	0.014	0.36	2.32	0.98
72768	0.09	0.44	0.011	0.011	0.38	2.22	0.95
72871	0.13	0.50	0.022	0.016	0.33	2.27	0.99
X6216	0.11	0.46	0.015	0.011	0.27	2.20	1.03

commercial practice is to use a continuous-annealing furnace that contains different temperature zones. The tubes are continuously moved through the furnace, from a zone that is maintained at the austenitizing temperature into a zone that is held constant at the isothermal anneal temperature.

For the four tubing heats studied, the austenitizing temperature was 857°C (for approximately 0.75 hr) and the isothermal hold temperature was 677°C, after which the tubes were air cooled (unfortunately, we were not able to determine how long they were held at 677°C or whether the procedure was the same for each heat). To remove residual stresses, we annealed three of the specimens for 0.25 hr at 650°C before aging; heat 72871 was tempered 1 hr at 704°C.

Tensile specimens were encapsulated in stainless steel containers and aged at 454, 510, and 566°C for 1000, 2500, 5000, 10,000, and 20,000 hr. The specimens were of the buttonhead type with a 3.18-mm (0.125-in.) diameter and a 28.6-mm (1.125-in.) gage section. Tensile tests were made on an Instron test machined at room temperature and the aging temperature at a nominal strain rate of 0.0007/s (crosshead speed: 0.02 mm/s).

Creep-rupture tests were made in air on lever-arm creep machines at 454, 510, and 566°C. During test, the specimens were heated with a resistance tube furnace, and the temperature was monitored and controlled by three Chromel vs Alumel thermocouples attached on the specimen gage length. Temperatures were controlled to ±1°C with a temperature variation

along the gage length of less than ±3°C. Elongation was determined with a mechanical extensometer attached to the specimen grips, and the specimen elongation was read periodically on a dial gage.

RESULTS

Microstructure

The unaged microstructures were primarily proeutectoid ferrite with about 20% bainite (Table 2 and Fig. 1); the bainite is the dark-etching constituent in Fig. 1. Two types of proeutectoid ferrite grains were observed: most ferrite grains contained a noticeable precipitate, while a few appeared barren. These details are more easily seen at a higher magnification [Figs. 2(a) and 3(a) for heats 72768 and X6216]. At these high magnifications, the dark-etching bainite often has a lamellar appearance, suggesting pearlite. In a previous report, we showed why this is not pearlite, but upper bainite.[6]

When the specimens were aged at 566°C, the precipitate microstructure continuously evolved toward a spheroidized structure. Precipitates formed and grew in the proeutectoid ferrite phase, while the carbides of the bainite gradually dissolved. The carbon and substitutional atoms then reappeared in spherical precipitate particles (Figs. 2 and 3). The evolution of the bainite was best observed in heat 72768 (Fig. 2). After 1000 hr, a lamellar structure was even more evident than in the unaged

Table 2. Microstructural Information for As-Received Tubing

Heat	Bainite[a] (%)	Grain Size (ASTM)	Microhardness[b] (DPH)
36202	26	8	143
72768	22	9	157
72871	17	8	149
X6216	22	8	163

[a]Balance is proeutectoid ferrite.

[b]Average of four determinations.

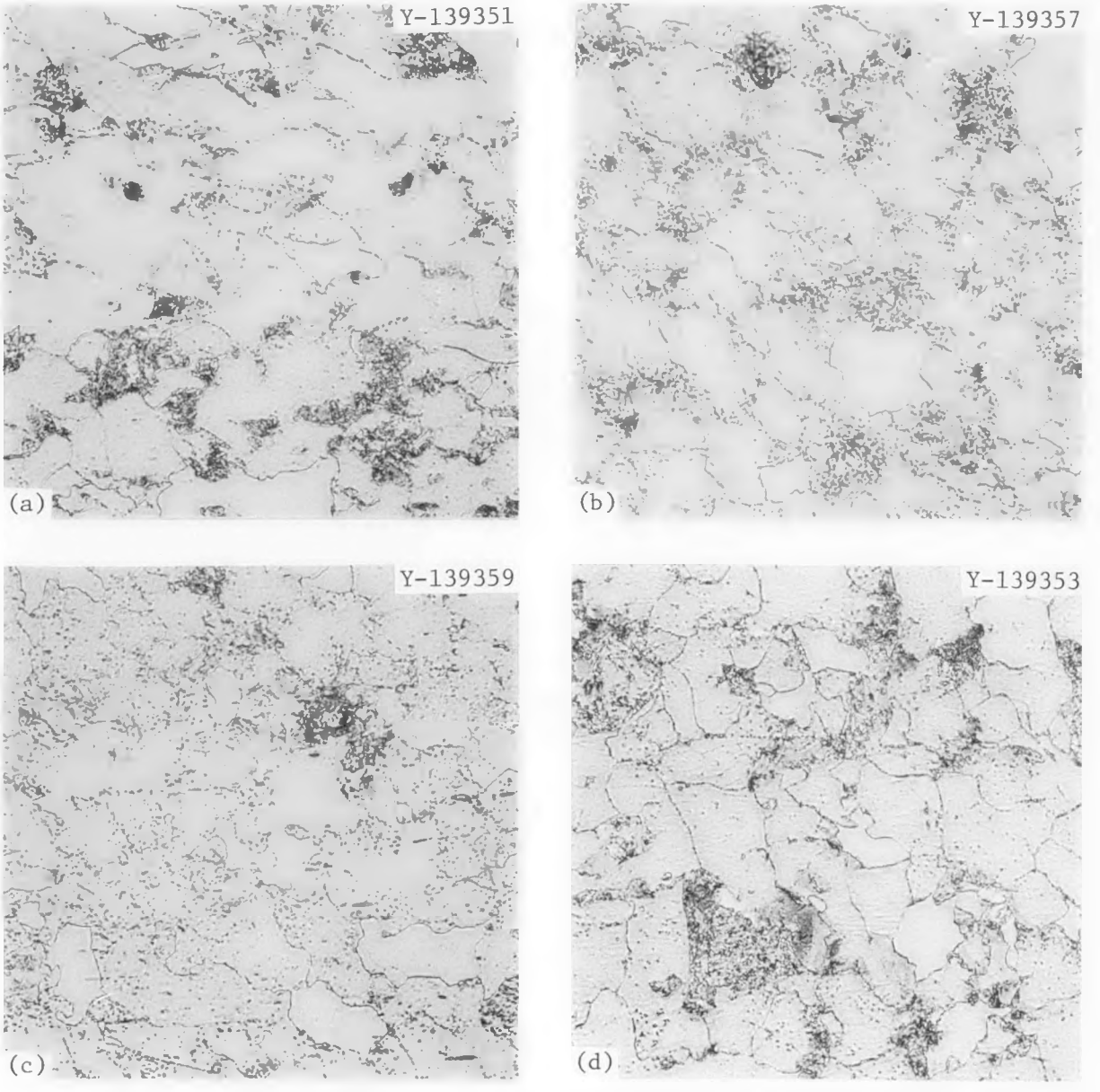

Fig. 1. Microstructures of Unaged Commercial Tubing Heats. 500×. (a) 36202. (b) 72768. (c) 72871. (d) X6216.

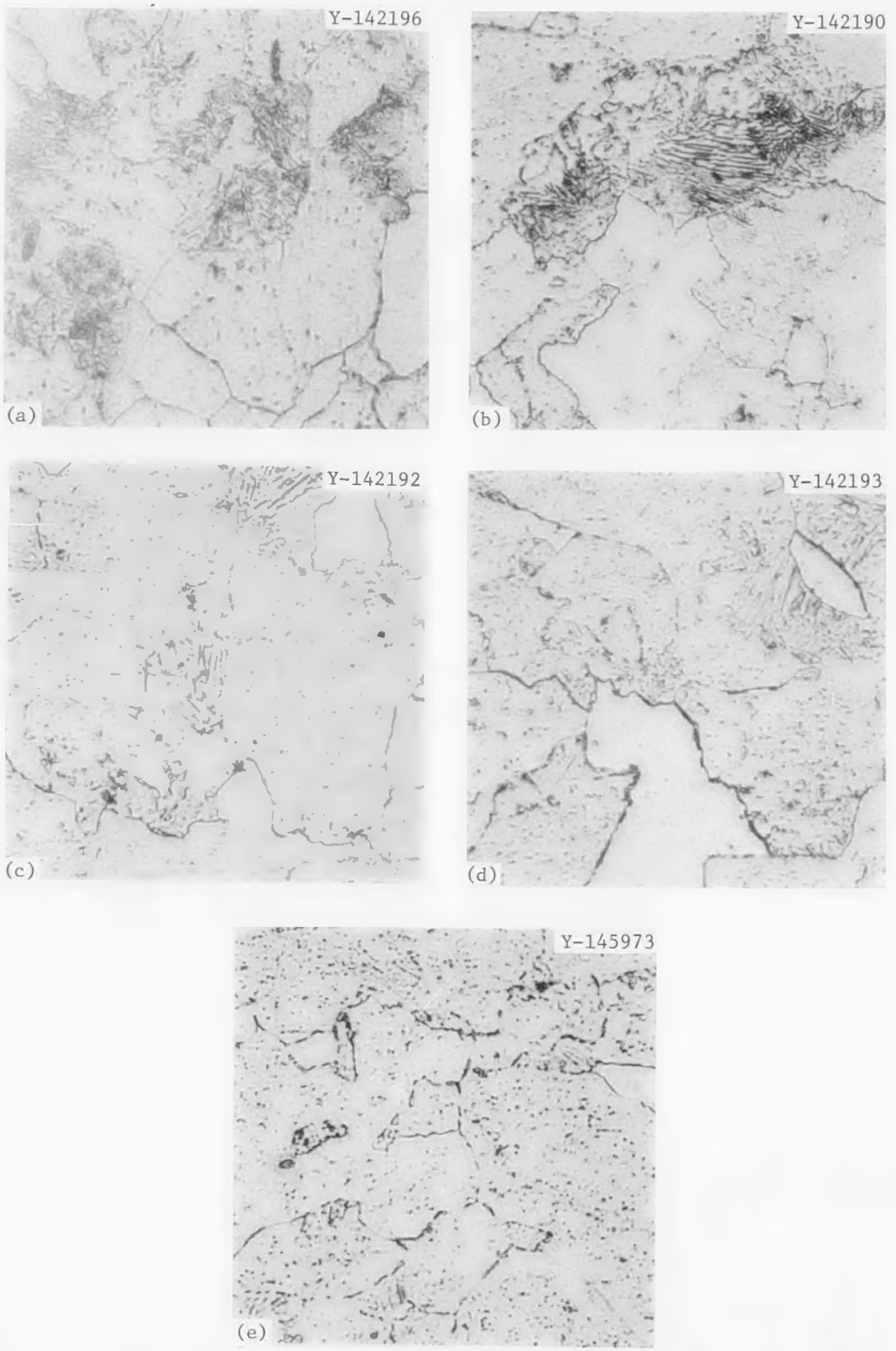

Fig. 2. Microstructure of Heat 72768 Aged for (a) 0, (b) 1000, (c) 5000, (d) 10,000, and (e) 20,000 hr at 566°C. 1500×. Reduced 16%.

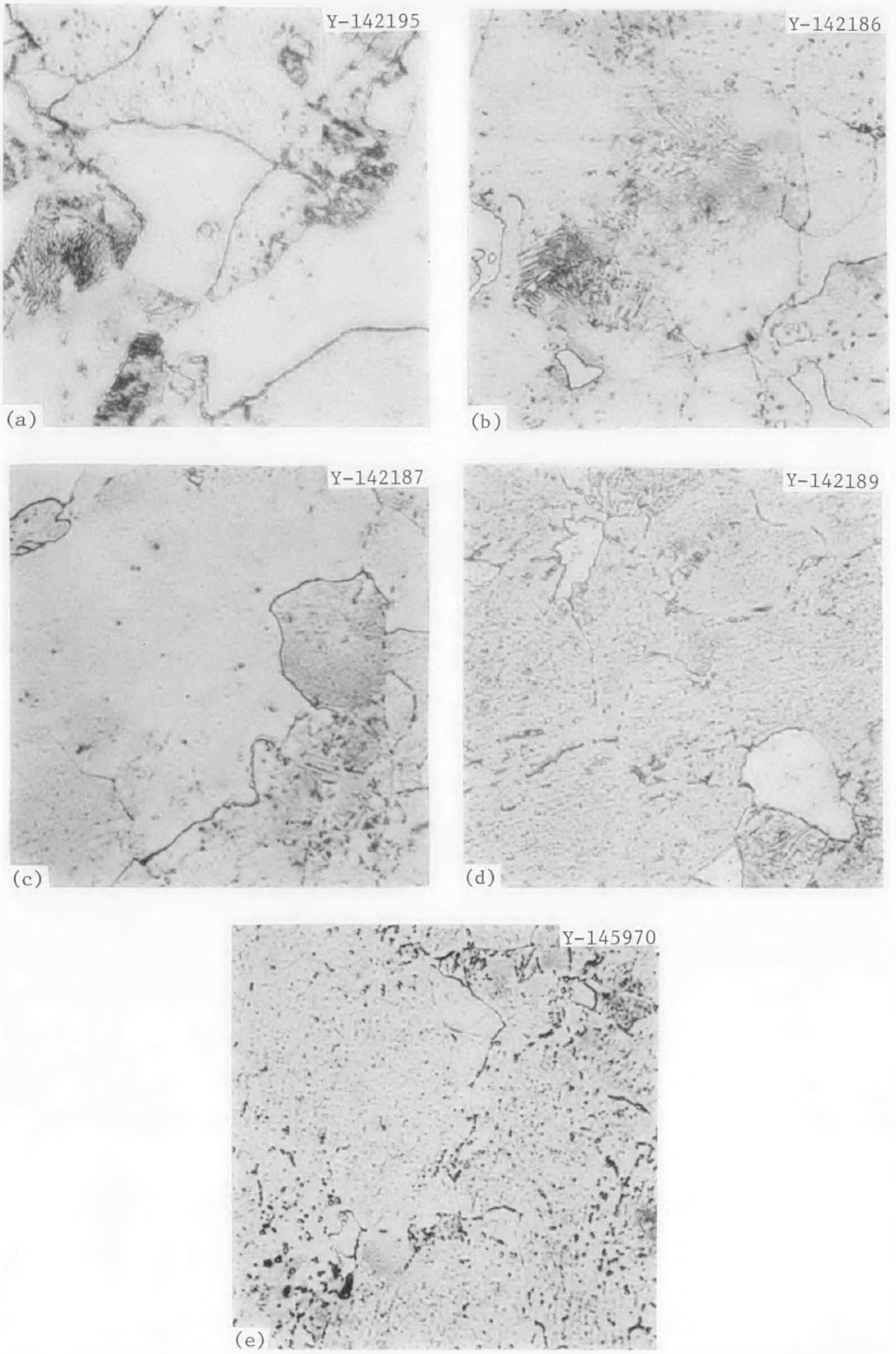

Fig. 3. Microstructure of Heat X6216 Aged for (a) 0, (b) 1000, (c) 5000, (d) 10,000, and (e) 20,000 hr at 566°C. 1500×. Reduced 16%.

steel [Fig 2(b)]. Evidently, large carbide platelets had grown at the expense of small ones (Ostwald ripening). By 10,000 hr, the evidence for bainite became indistinct [Fig. 2(d)]; by 20,000 hr, the tendency toward a spherical microstructure was even more evident [Fig. 2(e)]. A similar sequence of events occurred in heat X6216 (Fig. 3), but not as rapidly. As Figs. 2 and 3 illustrate, there were differences between heats 72768 (Fig. 2) and X6216 (Fig. 3). At all aging times, there was a higher density of small precipitate particles in the proeutectoid ferrite of X6216 than 72768, and the bainite redistribution was slower in X6216. A comparison of the microstructures of X6216 and 72768 with the other two heats indicated that the precipitate distribution in 36202 was similar to X6216 and that of 72871 was similar to 72768.

At 454 and 510°C, microstructural changes similar to those at 566°C occurred, but at reduced rates. From visual estimates, it appeared that somewhere between 5000 and 10,000 hr at 510°C, the microstructure approached that obtained after 1000 hr at 566°C. Even after 20,000 hr at 454°C, there was little noticeable difference from the unaged microstructure. The temperature effect was best seen by examining the microstructures at each temperature after 20,000 hr (Figs. 4—7).

Microhardness was measured on the undeformed portion of room-temperature tensile specimens (Table 3). At 566°C, the hardness changes were quite small: the hardnesses of heats 72871, X6216, and 72768 generally decreased with aging time, and 36202 initially increased, then gradually decreased. At 454 and 510°C, hardness changes showed considerable variation among the different heats: heats 72768 and 72871 showed only a small change; heat 36202 increased during the first 5000 hr, decreased between 5000 and 10,000 hr, then increased again after 20,000 hr; heat X6216's hardness peaked at 10,000 hr.

Tensile Properties

Tensile tests were made on all four heats at room temperature (Table 4) and at the aging temperature (Table 5) after aging for 1000, 2500, 5000, 10,000, and 20,000 hr. Strength changes due to aging depended not only on the aging time and temperature, but also on the test conditions.

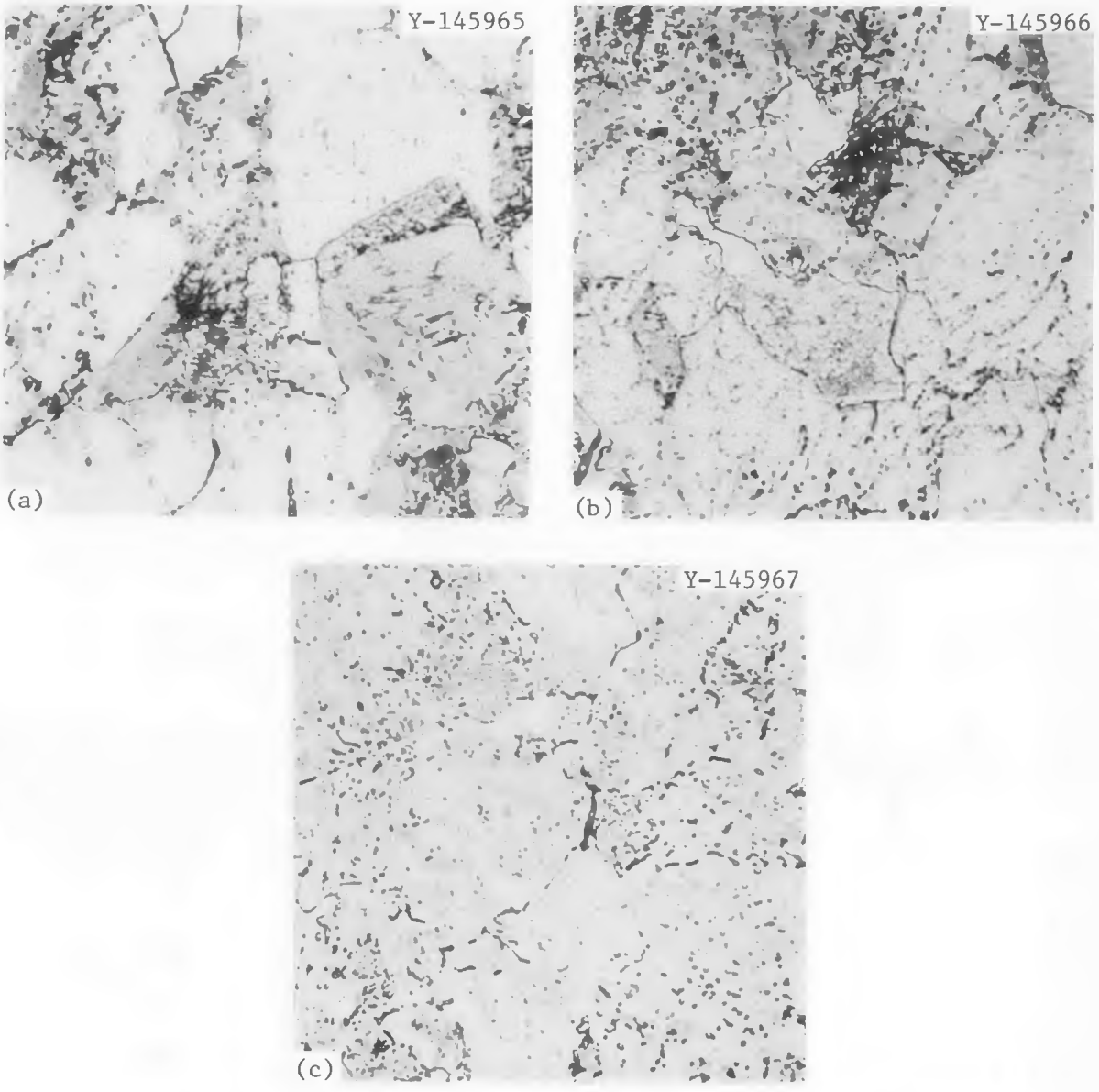

Fig. 4. Microstructure of Heat 36202 After Aging for 20,000 hr at (a) 454, (b) 510, and (c) 566°C. 1500×.

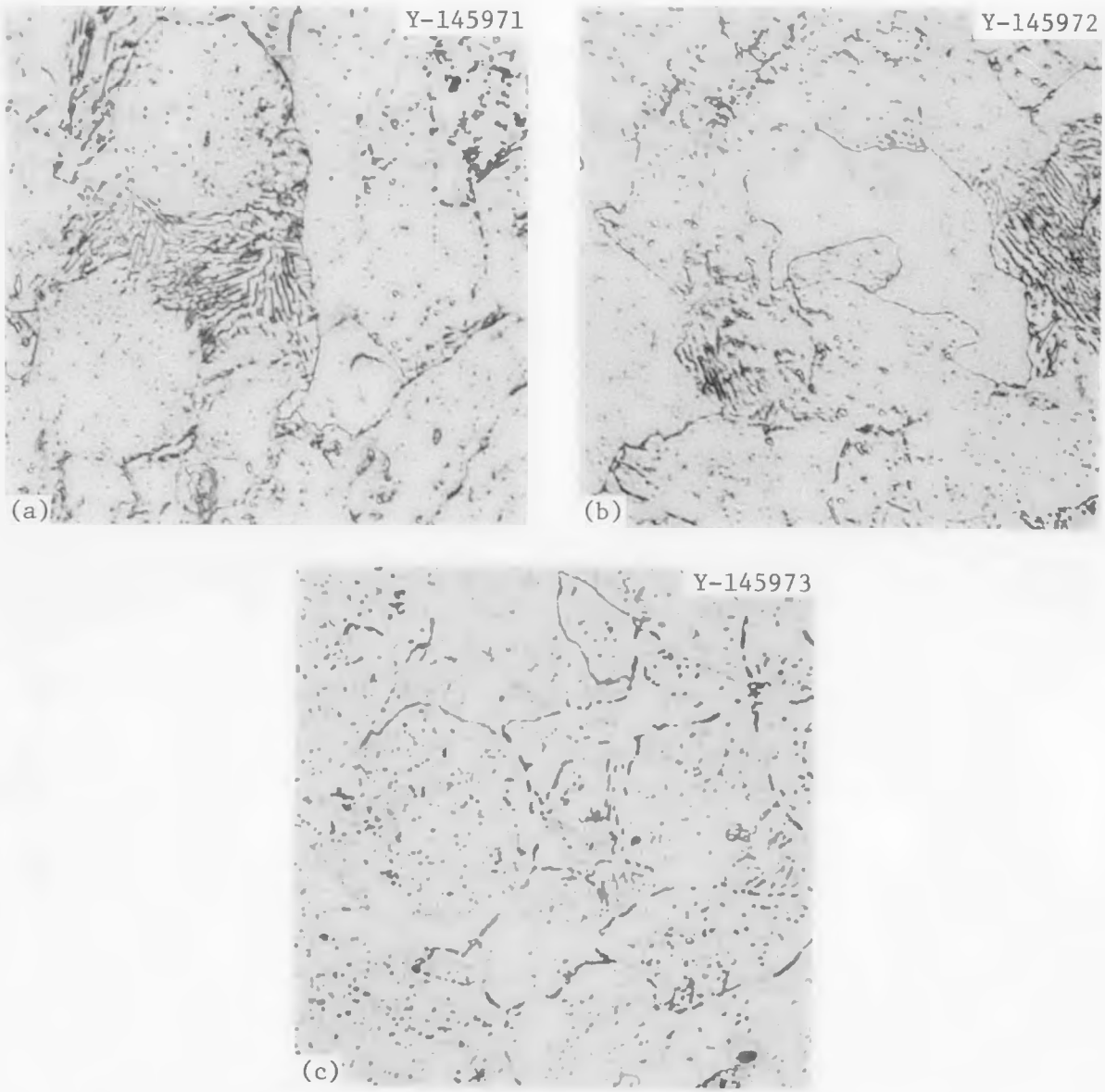

Fig. 5. Microstructure of Heat 72768 After Aging for 20,000 hr at (a) 454, (b) 510, and 566°C. 1500×.

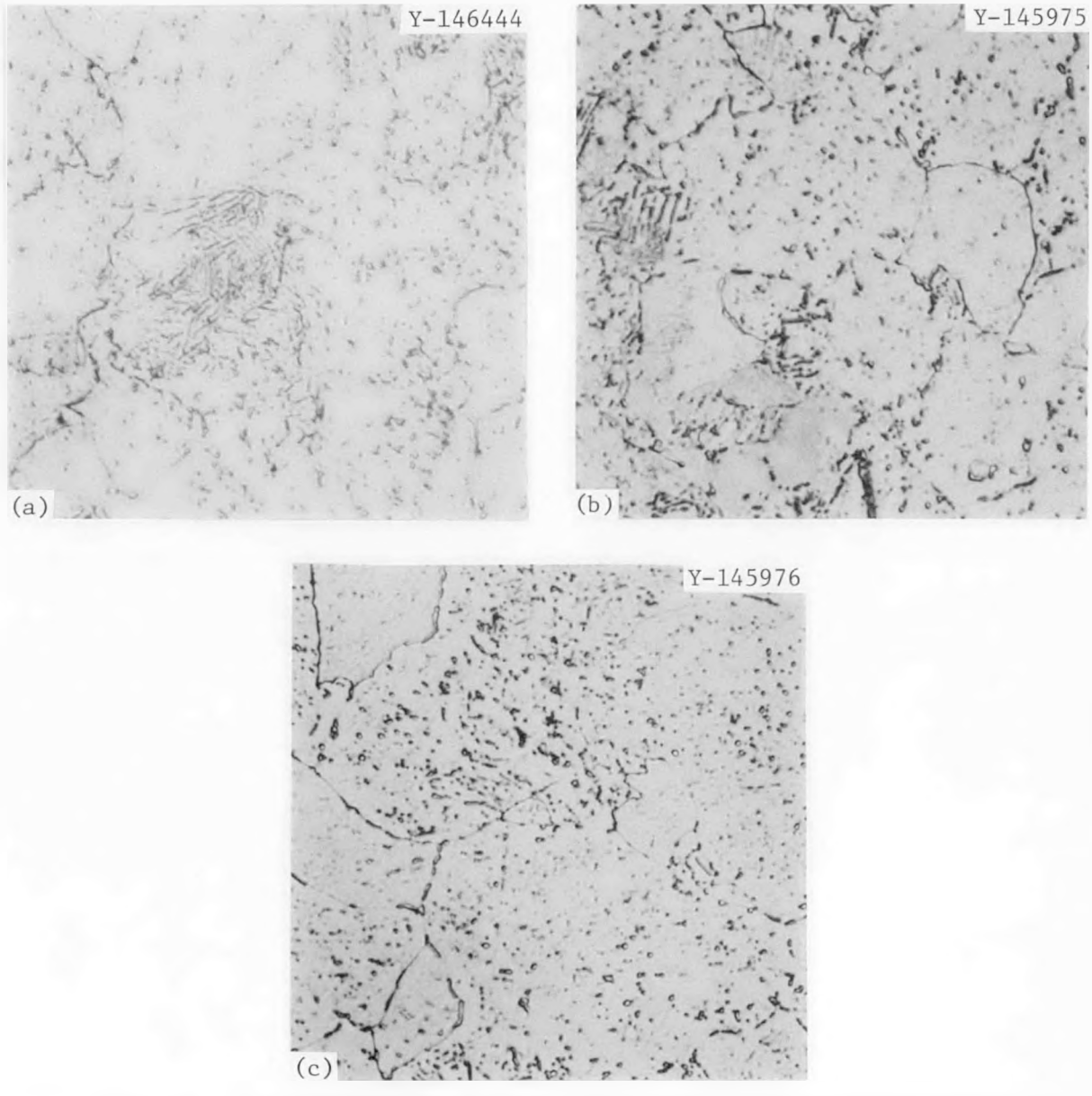

Fig. 6. Microstructure of Heat 72871 After Aging for 20,000 hr at (a) 454, (b) 510, and (c) 566°C. 1500×.

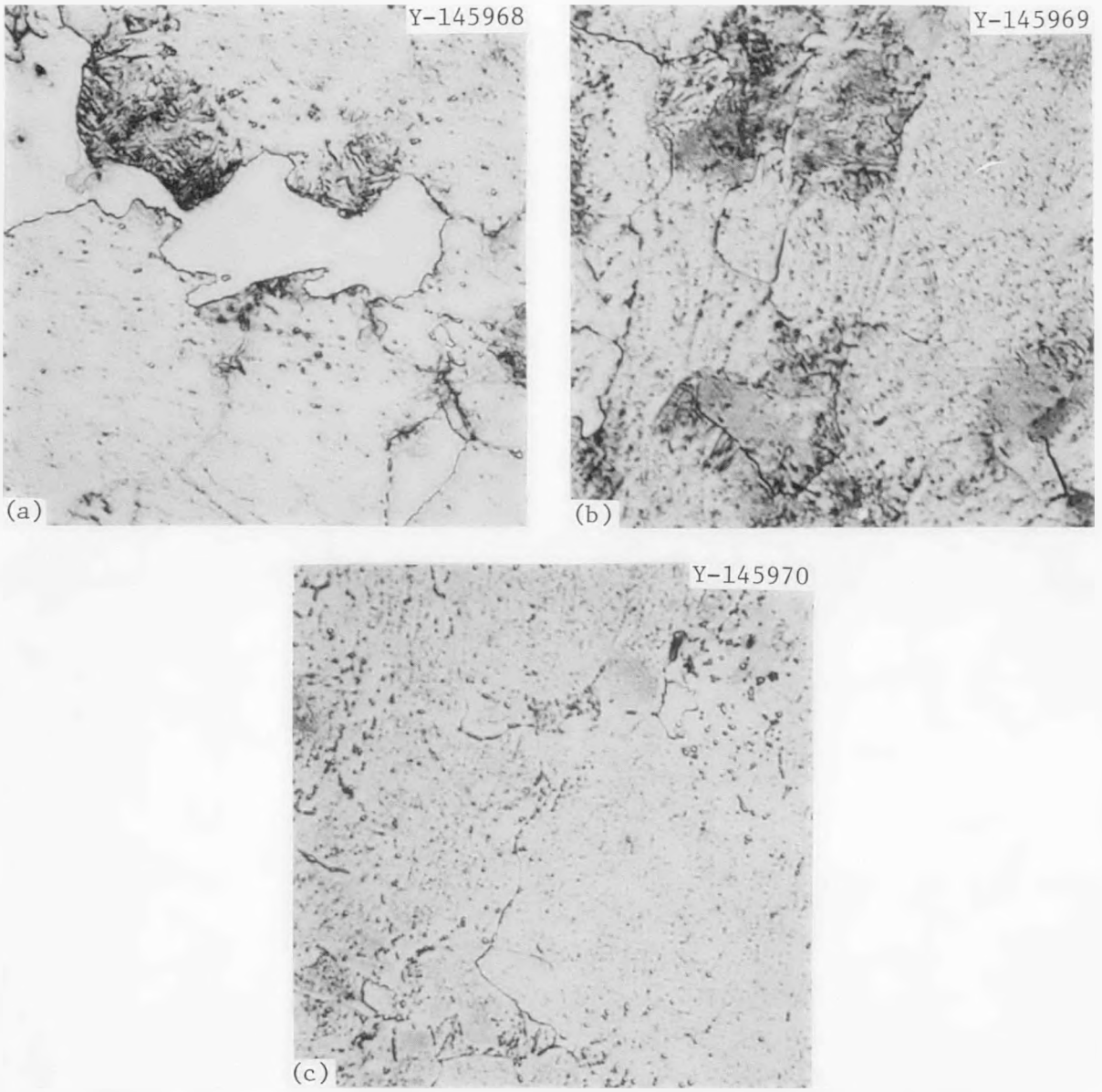

Fig. 7. Microstructure of Heat X6216 After Aging for 20,000 hr at (a) 454, (b) 510, and (c) 566°C. 1500×.

Table 3. Microhardness Changes of Aged Tubing Heats

Heat	Microhardness,[a] DPH, After					
	0 hr	1000 hr	2500 hr	5000 hr	10,000 hr	20,000 hr
			Aged at 454°C			
36202	143	162	164	165	161	167
72768	157	136	136	138	144	142
72871	149	155	141	143	142	144
X6216	163	156	153	153	167	154
			Aged at 510°C			
36202	143	167	165	169	161	165
72768	157	162	141	136	143	140
72871	149	146	149	147	147	141
X6216	163	162	165	156	166	156
			Aged at 566°C			
36202	143	166	160	159	142	148
72768	157	141	137	125	135	134
72871	149	144	144	143	140	137
X6216	163	163	150	152	152	146

[a]Average value from three hardness impressions.

Table 4. Room-Temperature Tensile Properties of Aged Commercial Tubing Heats of 2 1/4 Cr-1 Mo Steel

Aging Temperature (°C)	Aging Temperature (°F)	Aging Time (hr)	Strength, MPa (ksi) Yield	Ultimate	Fracture	Elongation, % Uniform	Total	Reduction of Area (%)
			Heat 36202					
		0	299 (43.4)	504 (73.1)	276 (40.0)	14.4	23.7	76.4
454	850	1,000	319 (46.3)	570 (82.7)	399 (49.2)	12.4	22.0	71.0
		2,500	323 (46.9)	577 (83.7)	337 (48.9)	11.7	21.9	72.1
		5,000	327 (47.4)	574 (83.3)	330 (47.9)	12.1	23.8	73.0
		10,000	294 (42.6)	548 (79.6)	316 (45.9)	11.4	22.6	70.8
		20,000	351 (50.9)	588 (85.3)	353 (51.2)	11.8	21.3	67.6
510	950	1,000	322 (46.8)	576 (83.6)	340 (49.3)	11.2	21.4	71.9
		2,500	312 (45.3)	573 (83.1)	326 (47.3)	11.0	21.3	73.8
		5,000	294 (42.7)	573 (83.2)	329 (47.7)	10.9	21.0	72.7
		10,000	266 (38.6)	546 (79.2)	312 (45.3)	12.4	22.6	70.6
		20,000	305 (44.3)	582 (84.5)	336 (48.7)	10.0	20.2	70.5
566	1050	1,000	325 (47.1)	572 (83.0)	322 (46.8)	10.9	21.6	72.8
		2,500	282 (40.9)	566 (82.1)	314 (45.6)	10.1	21.5	72.9
		5,000	271 (39.4)	555 (80.6)	314 (45.6)	11.7	22.3	74.6
		10,000	230 (33.4)	510 (74.0)	285 (41.3)	13.3	23.4	68.4
		20,000	239 (34.7)	528 (76.7)	302 (43.9)	13.8	23.5	71.3
			Heat 72768					
		0	339 (49.2)	548 (79.6)	314 (45.4)	13.0	22.7	69.3
454	850	1,000	244 (35.4)	487 (70.7)	285 (41.4)	14.3	24.9	74.6
		2,500	237 (34.4)	488 (70.8)	285 (41.4)	15.1	25.0	74.7
		5,000	232 (33.6)	486 (70.5)	280 (40.7)	14.8	24.4	73.0
		10,000	254 (36.8)	493 (71.6)	283 (41.1)	14.0	24.0	71.6
		20,000	245 (35.5)	494 (71.7)	285 (41.4)	15.2	25.5	72.3
510	950	1,000	287 (41.6)	544 (79.0)	313 (45.5)	13.0	23.0	70.5
		2,500	234 (34.0)	491 (71.3)	285 (41.4)	16.3	24.5	70.5
		5,000	218 (31.7)	486 (70.6)	298 (40.6)	14.7	24.9	70.5
		10,000	224 (32.5)	481 (69.8)	278 (40.4)	13.5	23.7	70.7
		20,000	223 (32.4)	501 (72.7)	289 (41.9)	14.3	23.5	70.5
566	1050	1,000	241 (35.0)	492 (71.4)	282 (41.0)	14.5	24.6	73.0
		2,500	222 (32.2)	493 (71.6)	285 (41.4)	14.1	24.5	71.4
		5,000	212 (30.7)	491 (71.2)	277 (40.2)	15.9	23.6	73.0
		10,000	205 (29.7)	473 (68.6)	265 (38.4)	13.4	24.2	73.2
		20,000	206 (29.9)	489 (71.0)	275 (39.9)	13.8	24.2	73.0
			Heat 72871					
		0	319 (46.3)	500 (72.5)	280 (40.6)	14.6	25.3	73.0
454	850	1,000	305 (44.2)	514 (74.6)	288 (41.8)	13.1	24.0	74.5
		2,500	249 (36.1)	508 (73.8)	291 (42.3)	13.7	22.8	72.2
		5,000	236 (34.3)	508 (73.7)	285 (41.4)	14.0	23.9	73.0
		10,000	244 (35.4)	491 (71.3)	279 (40.5)	13.0	24.2	71.4
		20,000	251 (36.5)	511 (74.2)	292 (42.4)	14.1	24.6	68.6
510	950	1,000	258 (37.5)	511 (74.1)	293 (42.5)	13.9	23.9	73.7
		2,500	234 (34.0)	509 (73.9)	287 (41.6)	13.8	23.9	73.8
		5,000	223 (32.4)	503 (73.0)	283 (41.1)	14.2	24.6	73.8
		10,000	229 (33.2)	486 (70.5)	277 (40.2)	13.9	24.6	73.3
		20,000	227 (32.9)	510 (74.0)	285 (41.4)	14.4	24.3	68.8
566	1050	1,000	245 (35.5)	515 (74.8)	289 (42.0)	13.8	24.1	73.8
		2,500	238 (34.6)	508 (73.8)	284 (41.2)	12.9	22.5	75.4
		5,000	225 (32.6)	506 (73.4)	284 (41.2)	13.0	23.8	73.5
		10,000	207 (30.1)	470 (68.2)	260 (37.8)	13.4	23.8	77.0
		20,000	215 (31.2)	495 (71.8)	280 (40.6)	14.7	25.0	70.5
			Heat X6216					
		0	353 (51.3)	562 (81.5)	324 (47.0)	12.4	20.0	71.1
454	850	1,000	278 (40.3)	533 (77.3)	304 (44.1)	11.9	21.9	70.4
		2,500	276 (40.1)	531 (77.0)	302 (43.9)	12.6	22.3	71.3
		5,000	283 (41.1)	539 (78.2)	307 (44.5)	12.3	22.2	70.4
		10,000	330 (47.9)	566 (82.2)	324 (47.0)	12.1	21.1	70.9
		20,000	279 (40.5)	542 (78.6)	309 (44.8)	11.7	20.9	69.5
510	950	1,000	281 (40.9)	535 (77.7)	309 (44.8)	12.4	22.1	68.6
		2,500	274 (39.8)	537 (77.9)	300 (43.5)	11.7	20.4	69.3
		5,000	266 (38.6)	530 (76.9)	290 (42.1)	12.3	21.7	69.4
		10,000	304 (44.2)	562 (81.5)	310 (45.0)	10.8	20.4	66.4
		20,000	267 (38.7)	539 (78.2)	297 (43.1)	12.8	21.0	69.6
566	1050	1,000	305 (44.2)	557 (80.8)	310 (45.0)	11.0	20.5	72.9
		2,500	255 (37.0)	520 (75.4)	287 (41.7)	11.5	21.2	75.3
		5,000	251 (36.5)	522 (75.8)	286 (41.5)	12.7	21.5	77.0
		10,000	251 (36.5)	521 (75.6)	295 (42.8)	11.7	21.5	72.7
		20,000	251 (36.4)	525 (76.2)	301 (43.7)	12.0	22.8	70.4

Table 5. Aging-Temperature Tensile Properties of Aged Commercial Tubing Heats of 2 1/4 Cr-1 Mo Steel

Aging and Test Temperature (°C)	(°F)	Aging Time (hr)	Strength, MPa (ksi) Yield	Ultimate	Fracture	Elongation, % Uniform	Total	Reduction of Area (%)
			Heat 36202					
		0	207 (30.0)	449 (65.2)	207 (30.0)	9.2	18.0	72.3
454	850	1,000	263 (38.1)	495 (71.9)	275 (39.9)	11.0	18.9	68.6
		2,500	265 (38.5)	471 (68.3)	262 (38.0)	9.8	19.8	70.4
		5,000	262 (38.0)	461 (66.9)	255 (37.0)	11.2	20.5	70.5
		10,000	230 (33.4)	442 (64.2)	244 (35.4)	10.2	21.2	69.9
		20,000	263 (38.2)	470 (68.2)	258 (37.4)	10.4	20.4	69.6
		0	209 (30.3)	422 (61.2)	174 (25.2)	9.1	19.7	80.0
510	950	1,000	251 (36.5)	420 (60.9)	194 (28.1)	9.5	23.2	76.9
		2,500	244 (35.4)	391 (56.8)	179 (26.0)	9.0	22.7	77.8
		5,000	234 (33.9)	380 (55.1)	181 (26.3)	8.4	23.8	76.8
		10,000	214 (31.0)	365 (53.0)	170 (24.7)	10.0	26.1	74.7
		20,000	234 (33.9)	378 (54.9)	179 (26.0)	7.9	26.5	74.7
		0	199 (28.9)	347 (50.3)	123 (17.8)	11.1	26.4	84.7
566	1050	1,000	224 (32.5)	326 (47.3)	118 (17.1)	8.2	31.7	82.8
		2,500	205 (29.8)	306 (44.4)	113 (16.4)	7.4	29.7	81.2
		5,000	196 (28.5)	294 (42.7)	110 (16.0)	7.4	35.4	80.5
		10,000	162 (23.5)	260 (37.7)	86 (12.5)	8.5	35.8	84.8
		20,000	170 (24.7)	265 (38.4)	87 (12.6)	7.6	34.2	82.1
			Heat 72768					
		0	229 (33.2)	480 (69.6)	254 (36.8)	10.0	18.2	68.8
454	850	1,000	223 (32.4)	447 (64.9)	244 (35.4)	10.6	19.6	75.4
		2,500	216 (31.4)	420 (60.9)	230 (33.4)	10.5	20.2	73.8
		5,000	173 (25.1)	382 (55.5)	213 (30.9)	11.3	22.1	74.6
		10,000	198 (28.8)	411 (59.6)	222 (32.3)	11.4	20.9	67.2
		20,000	186 (27.0)	404 (58.6)	218 (31.6)	12.2	21.5	71.4
		0	221 (32.1)	431 (62.6)	192 (27.8)	8.4	20.1	73.7
510	950	1,000	182 (26.4)	379 (55.0)	174 (25.2)	12.1	24.3	73.9
		2,500	214 (31.0)	358 (52.1)	162 (23.5)	10.6	26.5	78.6
		5,000	168 (24.4)	316 (45.8)	140 (20.3)	10.3	28.1	77.8
		10,000	182 (26.4)	329 (47.8)	145 (21.0)	9.8	28.6	78.0
		20,000	170 (24.7)	326 (47.3)	152 (22.0)	11.2	26.8	77.7
		0	203 (29.4)	348 (50.5)	123 (17.8)	10.1	29.2	82.8
566	1050	1,000	189 (27.5)	298 (43.3)	106 (15.4)	7.6	33.7	81.4
		2,500	184 (26.7)	287 (41.6)	112 (16.3)	7.3	32.7	82.7
		5,000	149 (21.6)	258 (36.4)	76 (11.1)	8.8	36.3	83.3
		10,000	145 (21.1)	238 (34.5)	74 (10.7)	7.6	34.3	83.9
		20,000	140 (20.3)	241 (35.0)	72 (10.5)	8.0	38.6	84.1
			Heat 72871					
		0	208 (30.2)	464 (67.4)	241 (35.0)	9.7	18.0	69.5
454	850	1,000	198 (28.7)	424 (61.6)	227 (33.0)	11.1	20.8	72.9
		2,500	192 (27.8)	395 (57.3)	213 (30.9)	10.9	21.5	73.0
		5,000	187 (27.1)	385 (55.9)	209 (30.4)	10.7	21.7	74.4
		10,000	194 (28.2)	389 (56.5)	207 (30.0)	10.6	22.4	73.3
		20,000	185 (26.9)	398 (57.7)	212 (30.8)	11.1	22.0	74.7
		0	204 (29.6)	409 (59.3)	174 (25.3)	9.0	21.0	79.2
510	950	1,000	182 (26.4)	356 (51.7)	152 (22.0)	11.5	26.9	79.9
		2,500	176 (25.6)	336 (48.8)	140 (20.3)	8.8	31.3	80.6
		5,000	167 (24.3)	336 (48.8)	152 (22.0)	9.9	29.0	82.0
		10,000	181 (26.2)	325 (47.2)	142 (20.6)	11.4	29.2	77.1
		20,000	177 (25.7)	331 (48.0)	145 (21.1)	9.6	30.0	77.9
		0	181 (26.2)	365 (47.2)	106 (15.4)	9.4	28.3	82.8
566	1050	1,000	165 (24.0)	282 (41.0)	88 (12.7)	10.4	33.1	89.2
		2,500	172 (24.9)	273 (39.6)	84 (12.2)	8.6	34.9	89.2
		5,000	165 (23.9)	262 (38.0)	76 (11.0)	8.2	39.3	89.7
		10,000	150 (21.8)	234 (33.9)	65 (9.5)	9.5	41.3	83.9
		20,000	148 (21.5)	247 (35.9)	70 (10.1)	9.5	46.6	85.3
			Heat X6216					
		0	291 (42.2)	516 (74.9)	265 (38.4)	8.7	16.6	71.2
454	850	1,000	282 (41.0)	492 (71.4)	257 (37.3)	9.5	18.5	70.3
		2,500	281 (40.9)	472 (68.5)	248 (36.0)	9.6	19.0	67.6
		5,000	240 (34.9)	430 (62.4)	227 (33.0)	9.9	20.4	73.0
		10,000	283 (41.1)	472 (68.5)	245 (35.6)	9.5	19.7	66.3
		20,000	236 (34.2)	448 (65.0)	241 (35.0)	11.0	21.5	69.5
		0	260 (37.8)	467 (67.8)	202 (29.3)	8.6	17.8	75.4
510	950	1,000	258 (37.4)	409 (59.3)	174 (25.3)	9.9	20.4	73.0
		2,500	240 (34.9)	373 (54.2)	147 (21.3)	9.2	23.4	80.5
		5,000	212 (30.7)	344 (49.9)	141 (20.5)	7.7	26.0	76.8
		10,000	255 (37.0)	393 (57.1)	167 (24.3)	7.9	22.2	76.3
		20,000	218 (31.7)	357 (51.8)	146 (21.2)	8.2	25.4	80.0
		0	254 (36.9)	391 (56.7)	147 (21.3)	8.7	23.5	79.9
566	1050	1,000	222 (32.2)	313 (45.4)	96 (13.9)	8.1	29.7	78.7
		2,500	184 (26.7)	274 (39.8)	76 (11.0)	7.9	37.4	84.6
		5,000	176 (25.5)	261 (37.9)	73 (10.6)	7.8	35.8	84.6
		10,000	171 (24.8)	269 (39.1)	77 (11.2)	7.9	30.8	85.0
		20,000	181 (26.2)	265 (38.5)	73 (10.6)	6.9	34.9	85.3

After 20,000 hr, the room-temperature yield strength generally showed a larger relative change than the ultimate tensile strength (Table 6). However, the yield strength for only heats 72768 and 72871 approached the minimum allowable value set for 2 1/4 Cr-1 Mo steel by ASTM or ASME Standards (207 MPa). This occurred after 20,000 and 10,000 hr at 566°C for 72768 and 72871 respectively. In no case was the minimum for the ultimate tensile strength (413 MPa) approached. Generally, the ultimate tensile strength showed a slight decrease after 20,000 hr. However, for heat 36202 aged 20,000 hr at 454 and 510°C the room-temperature yield strength and ultimate tensile strength were greater than those for the unaged steel; the ultimate tensile strength after aging at 566°C showed the same result. For 72871 the ultimate tensile strength after aging 20,000 hr at 454 and 510°C was greater than for the unaged steel, but the yield strength decreased significantly.

Table 6. Relative Change in Yield Strength (YS) and Ultimate Tensile Strength (UTS) After 20,000 hr

Aging Temperature (°C)	Relative Strength Change, %							
	36202		72768		72871		X6216	
	YS	UTS	YS	UTS	YS	UTS	YS	UTS
			Room-Temperature Tests					
454	+20	+16	−28	−10	−21	+2	−21	−4
510	+2	+15	−35	−9	−29	+2	−25	−4
566	−20	+5	−39	−12	−33	−1	−29	−7
			Aging Temperature Tests					
454	+27	+5	−19	−16	−14	−14	−19	−15
510	+12	−10	−23	−24	−13	−14	−16	−24
566	−15	−24	−31	−31	−18	−24	−29	−32

When tested at the aging temperature the changes in yield strength and ultimate tensile strength were significantly greater. With the exception of heat 36202, the ultimate tensile strength and yield strength showed similar changes — significant strength decreases. However, at 454°C the 36202 specimen aged for 20,000 hr was stronger than the unaged steel.

As indicated above, tensile behavior varied signficantly from heat to heat. Likewise, differences were noted as a function of aging time (Figs. 8 to 11). To aid in the interpretation of the data, smooth curves were fit through the tensile results for the elevated-temperature tests. Although curves have not been drawn through the room-temperature tests, the trends in all cases are similar to those for the elevated-temperature tests.

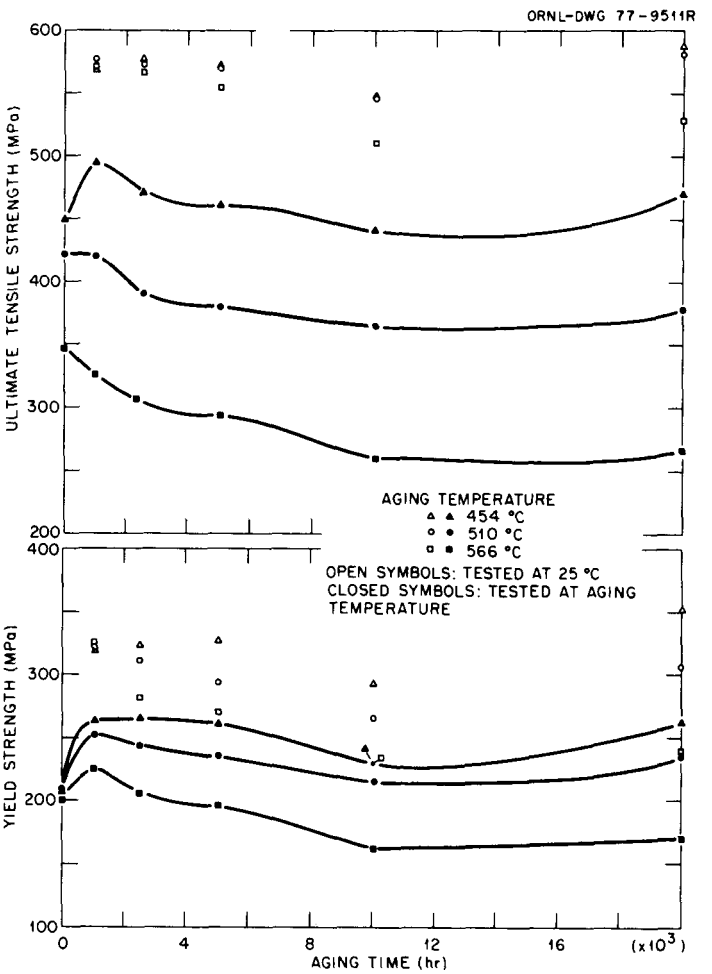

Fig. 8. Yield Strength and Ultimate Tensile Strength as Functions of Aging Time for Heat 36202. Trend Curves are shown for the aging-temperature tests.

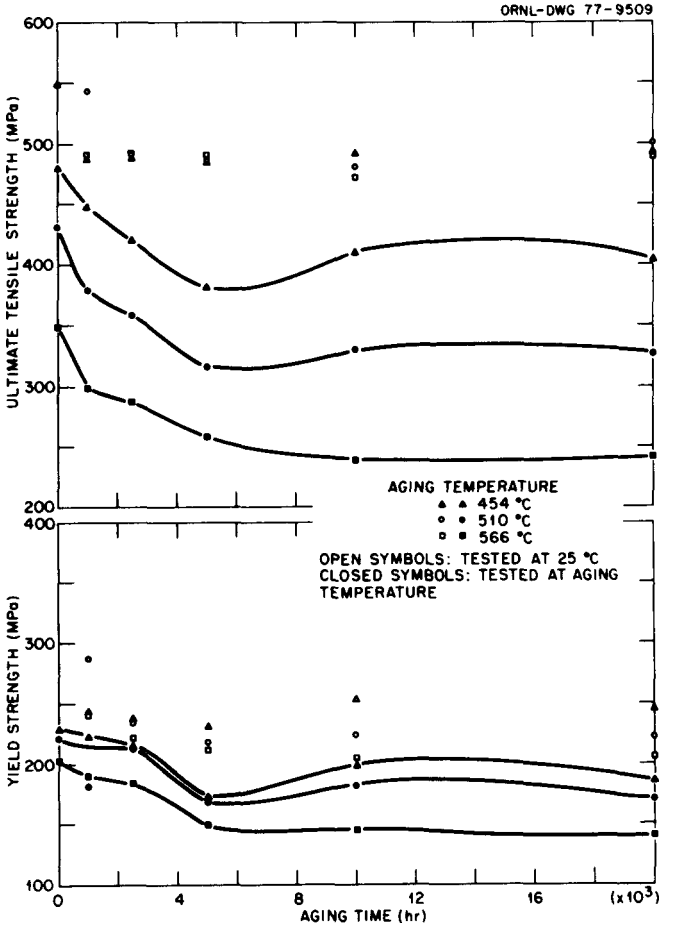

Fig. 9. Yield Strength and Ultimate Tensile Strength as Functions of Aging Time for Heat 72768. Trend curves are shown for the aging-temperature tests.

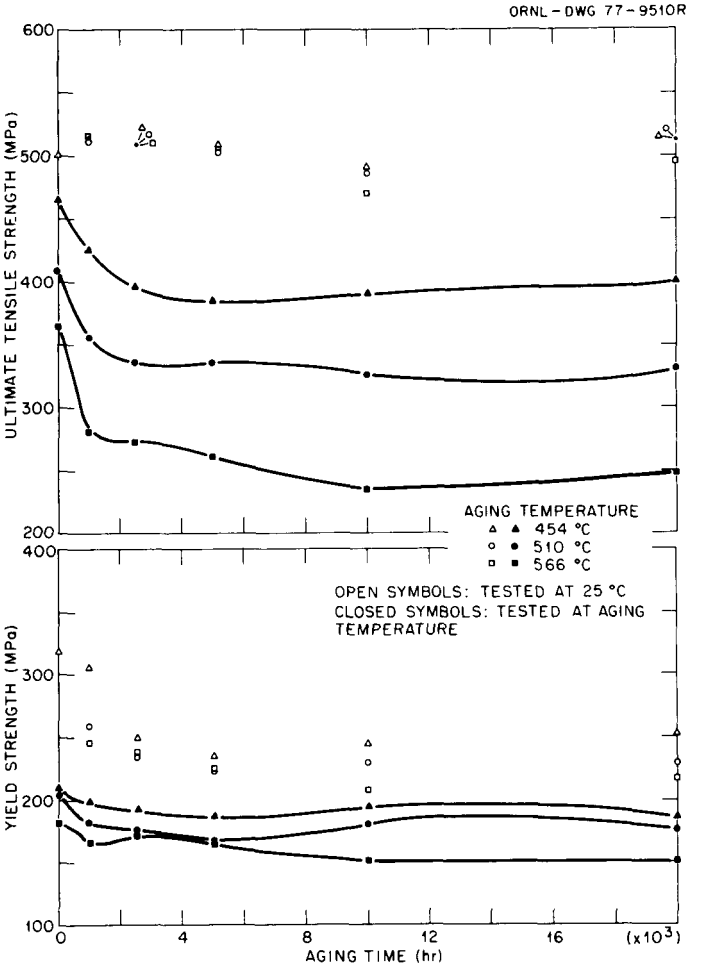

Fig. 10. Yield Strength and Ultimate Tensile Strength as Functions of Aging Time for Heat 72871. Trend curves are shown for the aging-temperature tests.

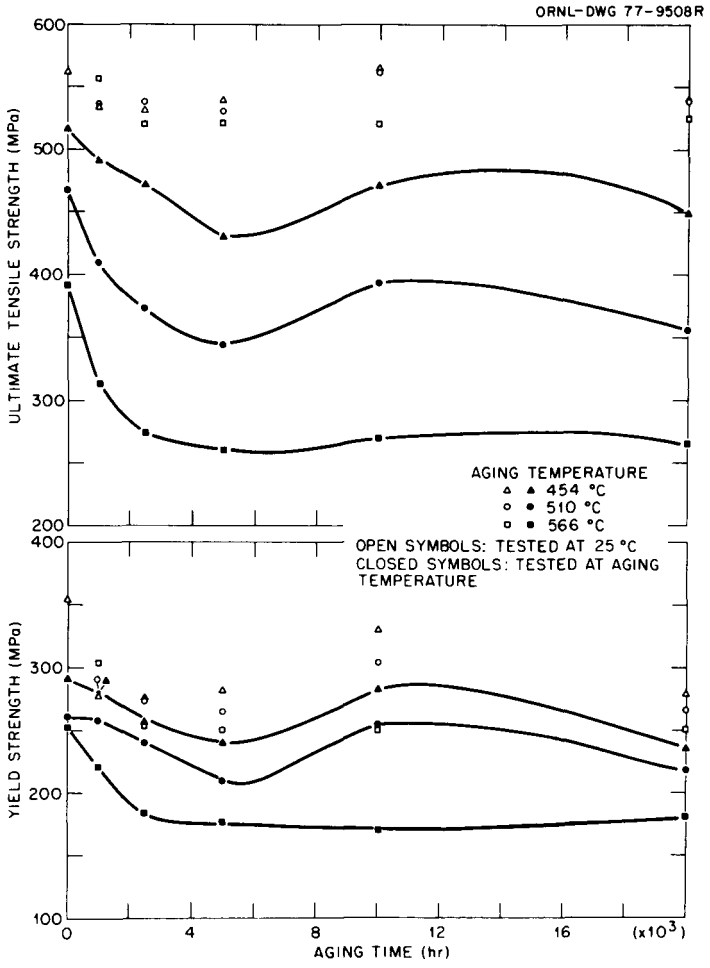

Fig. 11. Yield Strength and Ultimate Tensile Strength as Functions of Aging Time for Heat X6216. Trend curves are shown for the aging-temperature tests.

Since the strength trends followed by the yield strength and the ultimate tensile strength are similar, we will discuss the changes in the ultimate tensile strength. Heat 36202 (Fig. 8) had a strength peak for short aging times (<2500 hr). This peak was prominent at 454°C, subdued at 510°C, and nonexistent at 566°C (the peak was present in the yield strength behavior at 566°C). Instead of an early peak, the other three heats had a peak between 10,000 and 20,000 hr that was not present in heat 36202 (Figs. 9–11). However, the strength of heat 36202 increased between 10,000 and 20,000 hr, indicating that a peak may occur beyond 20,000 hr (Fig. 8).

In all four heats the effect of temperature was usually quite obvious. For example, the ultimate tensile strength for heat X6216 (Fig. 11) had very pronounced peaks at 454 and 510°C, but less pronounced at 566°C. Although the curves fit through the data points were rather arbitrary (e.g., no data were available between 10,000 and 20,000 hr), we can see that the lower the temperature, the higher the peak and the later it occurs. This is expected if the process that leads to the peak is diffusion-controlled, as expected for the precipitation reactions that give rise to the strength changes.

Changes in ductility generally paralleled strength changes (i.e., an increase in strength corresponded to a decrease in ductility). However, ductility in all cases showed only minor changes. For example, in only a few instances did the reduction of area fall below 70%.

Creep-Rupture Behavior

Only heats 72768 and X6216 were creep-rupture tested. When all specimens were tested under common conditions (138 MPa at 566°C), results (Tables 7 and 8) were qualitatively similar to those obtained in the elevated-temperature tensile studies (Fig. 12). That is, the relative maxima and minima in rupture life occurred at similar times during the aging process. Minimum creep rates correlate with the rupture times (i.e., a decrease in minimum creep rate corresponded to an increase in rupture life). For several tests, nonclassical curves of the type previously discussed for 2 1/4 Cr-1 Mo steel[7] were observed. These curves, which will be discussed further in the following section, have two steady-state stages (the creep rate for the second steady-state stage is given in Tables 7 and 8).

Table 7. Creep-Rupture Behavior of Heat X6216 of Aged 2 1/4 Cr-1 Mo Steel Tested at 138 MPa (20 ksi) and 566°C

Aging Time (hr)	Rupture Life (hr)	Total Elongation (%)	Reduction of Area (%)	Minimum Creep Rate (%/hr)
		Aged at 566°C		
0	2196.3	19.7	47.0	0.000333
1,000	1660.0	20.8	58.0	0.000485
2,500	521.5	37.1	75.3	0.0251
5,000	332.4	36.7	78.4	0.0447
10,000	172.1	35.6	83.0	0.0850
20,000	202.4	37.8	78.0	0.0728
		Aged at 510°C		
1,000	997.3	24.6	65.0	0.0108[a]
2,500	673.0	29.5	73.6	0.0170
5,000	685.8	36.2	69.4	0.0183
10,000	2294.0	19.5	49.0	0.00266
20,000	1338.8	23.0	53.8	
		Aged at 454°C		
1,000	936.6	29.2	70.9	0.0124[a]
2,500	881.7	24.9	70.3	0.0123[a]
5,000	832.5	25.4	70.5	0.0142[a]
10,000	2368.8	17.7	39.3	0.00323[a]
20,000	989.7	31.9	69.2	

[a]Creep curve had two steady-state stages; creep rate is that of second steady-state stage.

Table 8. Creep-Rupture Behavior of Heat 72768 of Aged 2 1/4 Cr-1 Mo Steel Tested at 138 MPa (20 ksi) and 566°C

Aging Time (hr)	Rupture Life (hr)	Total Elongation (%)	Reduction of Area (%)	Minimum Creep Rate (%/hr)
		Aged at 566°C		
0	406.8	52.0	70.3	0.0474[a]
1,000	193.6	54.8	81.9	0.110
2,500	116.6	54.6	84.1	0.188
5,000	90.0	50.6	79.9	0.235
10,000	35.1	53.6	53.6	0.702
20,000	37.0	50.0	80.6	0.610
		Aged at 510°C		
1,000	301.0	50.4	81.9	0.0632[a]
2,500	195.4	58.3	83.5	0.114
5,000	154.0	56.6	84.1	0.145
10,000	172.9	50.0	80.2	0.126
20,000	125.7	53.1	80.9	0.170
		Aged at 454°C		
1,000	389.3	44.6	77.8	0.0519[a]
2,500	301.7	57.4	80.7	0.0522
5,000	320.8	52.2	81.3	0.0532
10,000	314.5	48.7	82.3	0.0236
20,000	315.3	57.0	80.0	0.0277

[a]Creep curve had two steady-state stages; creep rate is that of second steady-state stage.

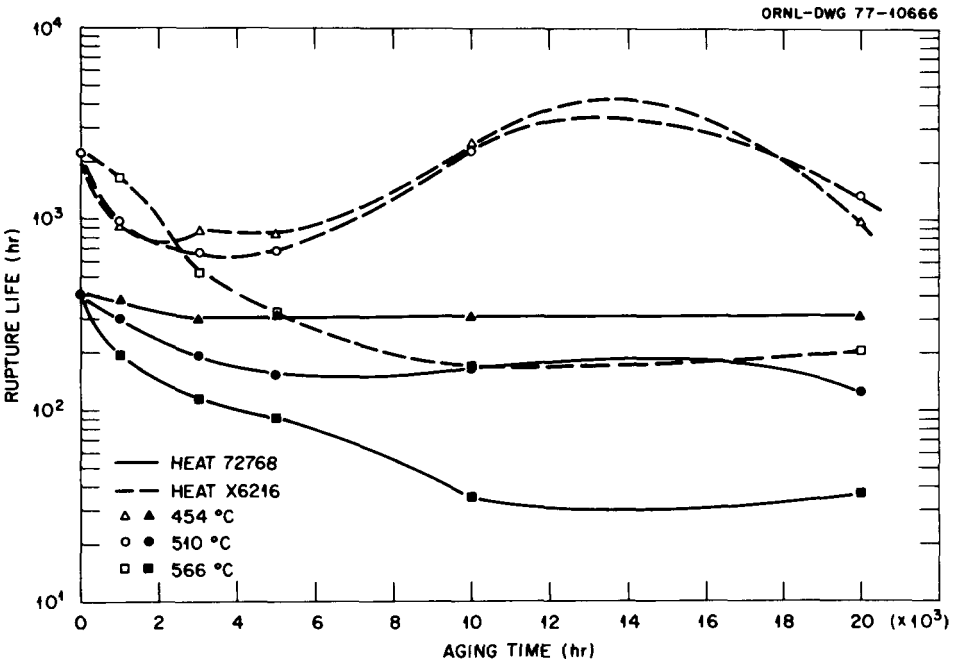

Fig. 12. Rupture Life as a Function of Aging Time for Heats 72768 and X6216 Tested at 138 MPa at 566°C.

Several tests were also made at 454 and 510°C on specimens aged at these temperatures. Heat 72768 (Table 9) was tested at 207 and 379 MPa at 510 and 454°C, respectively; heat X6216 (Table 10) was tested at 241 and 413 MPa at 510 and 454°C, respectively. Since only qualitative comparisons are possible, most of our discussion will be confined to tests made at 138 MPa at 566°C. Tests at the other aging temperature gave similar trends.

DISCUSSION

The complex aging behavior of 2 1/4 Cr-1 Mo steel is governed by complicated carbide precipitation processes in the steel. Baker and Nutting[1] investigated the precipitation reactions and concluded that they depend upon the microstructural constituent (i.e., different carbide reaction processes occur in bainite than in proeutectoid ferrite).

Table 9. Creep-Rupture Behavior of Heat X6216 of Aged 2 1/4 Cr-1 Mo Steel Tested at Aging Temperature

Aging Time (hr)	Rupture Life (hr)	Total Elongation (%)	Reduction of Area (%)	Minimum Creep Rate (%/hr)
	Tested and Aged at 510°C, 241 MPa			
0	3370.5	21.2	60.0	0.000730
1,000	1286.2	38.0	70.5	0.00506
2,500	63.0	40.4	79.2	0.295
5,000	38.1	34.6	77.8	0.438
10,000	398.8	36.6	75.2	0.0349
20,000	91.8	33.7	79.0	0.162
	Tested and Aged at 454°C, 413 MPa			
0	>5000[a]			0.000868
1,000	3274.4	19.6	60.2	0.00174
2,500	42.1	23.1	71.2	0.220
5,000	0.3	20.5	65.1	
10,000	70.4	22.0	66.9	0.115
20,000	5.5	22.7	76.0	1.33

[a]Test was discontinued after 3026 hr when test was just beginning tertiary creep; estimate of 5000 hr is probably conservative.

Table 10. Creep-Rupture Behavior of Heat 72768 of Aged 2 1/4 Cr-1 Mo Steel Tested at Aging Temperature

Aging Time (hr)	Rupture Life (hr)	Total Elongation (%)	Reduction of Area (%)	Minimum Creep Rate (%/hr)
	Tested and Aged at 510°C, 207 MPa			
0	2752.0	28.4	61.2	0.000538
1,000	1252.5	34.3	72.2	0.00797
2,500	207.2	43.9	80.0	0.108
5,000	100.4	45.4	76.3	0.0222
10,000	164.2	41.7	74.3	0.130
20,000	98.6	49.8	79.8	
	Tested and Aged at 454°C, 379 MPa			
0	1110.0	21.7	71.7	0.00632
1,000	357.8	21.3	64.0	0.0166
2,500	1.5	24.5	67.0	6.45
5,000	0.3	25.8	65.1	

In bainite, which makes up only a small portion of the microstructure of the steels tested, Baker and Nutting[1] found that M_3C and Mo_2C form quite early — usually during the heat treatment. During elevated-temperature exposure, these carbides are replaced by M_7C_3, $M_{23}C_6$, and eta-carbide. (In the literature, eta-carbide is usually referred to as M_6C.[1—3] Recent studies have shown that eta-carbide in aged 2 1/4 Cr-1 Mo steel more nearly approximates M_4C.)[8] The M_7C_3 is eventually replaced by eta-carbide, and the final microstructure evolves to a ferrite that contains $M_{23}C_6$ and eta-carbide.[1]

For proeutectoid ferrite, which makes up the greater part of the microstructure of annealed 2 1/4 Cr-1 Mo steel (the starting material for the present study), Mo_2C precipitates during the heat treatment and/or during elevated-temperature exposure.[1] However, this carbide is unstable and eventually gives way to eta-carbide. Since the microstructure of an annealed steel such as that used in these studies is not entirely proeutectoid ferrite, but also contains bainite and pearlite (Hale[2] found the carbides in pearlite to be $M_{23}C_6$), the microstructure of an annealed steel also evolves toward a ferrite that contains large globular particles of $M_{23}C_6$ and eta-carbide.[1,2,9] Since the proeutectoid ferrite microstructure determines the properties, this discussion will be confined to the processes that occur in this constituent.

The Mo_2C in proeutectoid ferrite forms as high a density of fine needles or platelets,[1,2] and investigators have concluded that it is the only precipitate that strengthens the alloy by dispersion hardening.[1,10] Although the large globular $M_{23}C_6$ and eta-carbide particles are concluded to afford little strengthening,[1,10] some recent results have shown that these particles can affect strength.[5] However, for this discussion, we will confine our remarks to precipitation strengthening by Mo_2C, since the effect of the globular particles occurs after longer aging times and for test conditions not used in this study.

In addition to precipitation strengthening in 2 1/4 Cr-1 Mo steel, there is also a solid solution strengthening effect that occurs. This effect gives rise to dynamic strain aging peaks in plots of flow stress

against temperature in unaged steel. For annealed 2 1/4 Cr-1 Mo steel, a plot of ultimate tensile strength against temperature has a dynamic strain aging peak near 350°C. Baird and Jamieson[11,12] concluded that this peak occurred by a process they termed "interaction solid solution hardening." Interaction solid solution hardening occurs in steels that contain in solution interstitial and substitutional solutes that have an affinity for each other.

Baird and Jamieson studied Fe-Mo-C and Fe-Cr-C alloys and showed that interaction solid solution hardening extended the dynamic strain aging peak to temperatures above those observed when dynamic strain aging is due to only carbon and/or nitrogen (this latter effect is confined to the range 100 to 300°C, the "blue brittleness" range). They concluded that the effect is the result of the formation of Mo-C and Cr-C atom pairs or atom clusters, which subsequently form dislocation atmospheres.[11] Since such a dislocation atmosphere is much less mobile than an atmosphere that contains only interstitial atoms, the strengthening effect is extended to higher temperatures before the atmosphere can migrate with a dislocation and thus not impede its motion. Baird and Jamieson found that interaction solid solution hardening also gave rise to strengthening during creep.[12]

In our studies on the tensile[13] and creep[7] behavior of 2 1/4 Cr-1 Mo steel, we extended the Baird and Jamieson[11,12] studies to explain our observations. For the annealed steel with microstructures that were primarily proeutectoid ferrite, we concluded that interaction solid solution hardening was due to Mo-C interactions. For the annealed steels used in the aging studies being discussed in this report, the microstructures were primarily proeutectoid ferrite (Table 2), and we will assume the properties are due to effects occurring in that constituent. Hence, only the Mo-C interactions will be considered.

The extent of interaction solid solution hardening depends on the precipitation that occurs in proeutectoid ferrite during annealing. When proeutectoid ferrite forms during heat treatment, is is supersaturated with molybdenum and carbon. Whether this supersaturation is relieved by Mo_2C precipitation during the heat treatment or during

elevated-temperature service depends upon how rapidly the steel is cooled after the proeutectoid ferrite forms. The more rapid the cooling, the more molybdenum and carbon remain in solution, and thus the larger the interaction solid solution hardening effect during subsequent elevated-temperature exposure. Alternatively, as the amount of molybdenum and carbon in solution is removed by precipitation, the strength of the dynamic strain aging peak decreases.[13]

It is interaction solid solution hardening that gives rise to nonclassical creep curves of the type found on unaged specimens[7,12] and specimens aged for only short periods of time (Tables 7 and 8). Baird and Jamieson[12] showed that dislocation motion in creep is hindered by atmospheres of molybdenum and carbon atom clusters. In annealed 2 1/4 Cr-1 Mo steel, this interaction gives rise to nonclassical creep curves in certain temperature and stress regimes.[7] Instead of a classical creep curve with a primary (transient), secondary (steady-state), and tertiary creep stage, a curve with two steady-state stages is observed. The transition from the first to the second steady-state stage involves a quasi-tertiary (increasing creep rate) creep stage.

The first of the steady-state stages in the nonclassical creep curves was concluded to be the result of interaction solid solution hardening.[7] With time, the amount of molybdenum and carbon in solution decreases (by precipitate formation) until the interaction no longer hinders dislocation motion. At this point, the creep rate increases and eventually establishes a new steady state with a higher creep rate, where creep is controlled by atmosphere-free dislocations moving through the Mo_2C precipitate field of the proeutectoid ferrite.

Tensile results for the four heats showed that properties varied considerably from heat to heat. This was evident when the unaged properties were examined[6] and also when the behavior for the different heats after aging was compared (Tables 4 and 5). There were apparently two kinds of hardening peaks, only one of which was found in any one alloy of this study. This behavior can be explained in terms of the hardening processes discussed above for proeutectoid ferrite. For this discussion we will refer to tensile behavior at the aging temperature (Figs. 8–11).

Heat 36202 was the only heat that displayed a strength peak during the first 1000 hr of aging (Fig. 8). This was evident only at 454°C for the ultimate tensile strength but at all temperatures for yield strength. Strengths for the other three heats (Figs. 9—11) decreased during the first 5000 hr, after which they increased. This resulted in a strength peak between 10,000 and 20,000 hr. Since no data were taken between 10,000 and 20,000 hr, we could not accurately detect the peak. It was not present in the data for heat 36202 (Fig. 8). However, the strength for this heat was apparently still increasing after 20,000 hr, indicating that the peak in this case occurs at longer aging times.

This range of aging behavior can perhaps best be understood by directly comparing the behavior of heats 36202 (Fig. 8) and X6216 (Fig. 11) at 454°C (Fig. 13). Although the strength characteristics of these two heats have some similarities (they are both stronger than the other two heats), they show significant differences during aging. The early peak of heat 36202 coincided with a continuously decreasing strength for X6216. Heat X6216 then went through a minimum, while the strength of heat 36202 decreased. Finally, heat X6216 went through a maximum between 10,000 and 20,000 hr, while the strength of heat 36202 began to increase to a maximum, probably beyond 20,000 hr. It was as though the strength-aging time curve for heat 36202 was displaced in time, the same processes occurring, but at later times. Although the maximum effect was noted at 454°C (Fig. 13), the same trends were apparent at the other temperatures, where the metallurgical processes that gave rise to these effects are speeded up.

These observations can be explained in terms of the strengthening processes discussed above. The early peak in heat 36202 must be the result of interaction solid solution hardening. For some reason, heat 36202 requires a longer time at temperature before the maximum strength is developed by this mechanism.

The maximum strength for heat X6216 due to this process must occur before the 1000-hr age, giving rise to the continuous strength decrease at early aging times. Since heats X6216 and 72768 both have

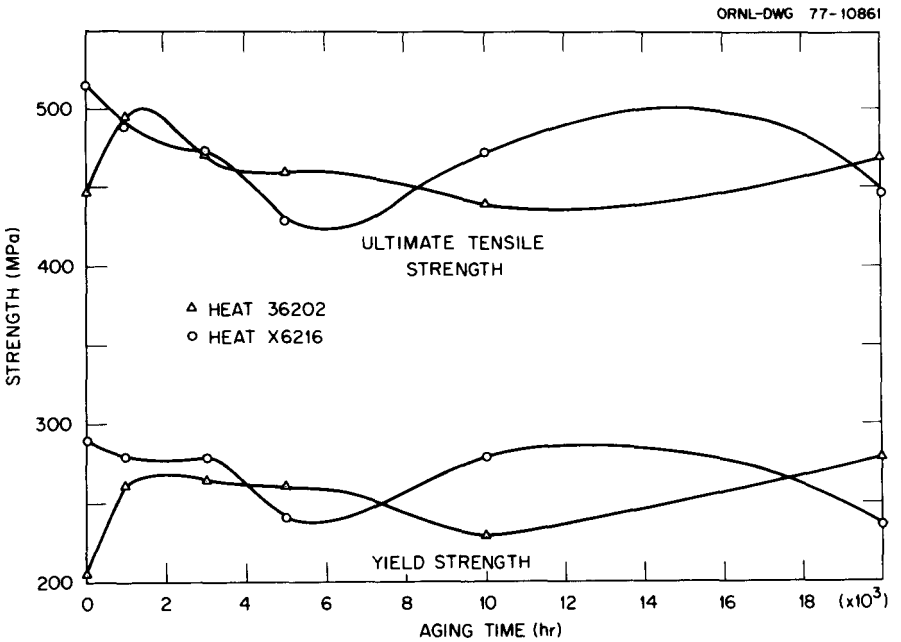

Fig. 13. A Comparison of the Yield Strength and Ultimate Tensile Strength as Functions of Aging Time for Heats 36202 and X6216 Tested at 454°C.

nonclassical creep curves after short aging periods, interaction solid solution hardening must also add to the strength in the other three heats, but optimum strengthening by this effect occurs earlier.

When the amount of molybdenum and carbon in solid solution decreases because of Mo_2C precipitation, interaction solid solution hardening is replaced by dispersion strengthening as the dominant strengthening mechanism. The resulting peak is delineated in the heat X6216 data (Fig. 13) but occurs beyond 20,000 hr for heat 36202. The peak is associated with some optimum precipitate size and density. Of course, some disperson-strengthening occurs throughout the aging process. However, as seen above, during the early stages interaction solid solution hardening is the dominant strengthening mechanism.

The behavior of heats 72768 and 72871 parallels that of X6216 in that the Mo_2C peaks can be delineated, but not the early peak due to interaction solid solution hardening. The Mo_2C peaks for these latter two heats are considerably smaller than for heat X6216 (Figs. 9 and 10).

The microstructures generally supported the above conclusions concerning dispersion strengthening by Mo_2C. Heats 72768 and 72871, the weakest heats, had a much lower precipitate density and larger precipitate particle size in the proeutectoid ferrite than the other two heats (Figs. 4–7). For most of the aging times at 454 and 510°C and for the shorter aging times at 566°C, these precipitates should be Mo_2C.[1] The lower precipitate densities give rise to lower strength, as observed.

One difficulty with the above explanations concerns the observations on unaged heats 36202 and X6216. Heat X6216 had a much higher room-temperature strength and developed a higher dynamic strain aging peak at about 370°C when the ultimate tensile strength was plotted against temperature.[6] Both heats had similar chemical compositions (Table 1). Since the early aging peak for heat 36202 (Fig. 13) that was attributed to interaction solid solution hardening takes longer to develop than for heat X6216, heat 36202 must contain considerable molybdenum and carbon in solution in the unaged condition. Hence, for similar test conditions we should expect the dynamic strain aging effect for unaged heat 36202 to be comparable to that of X6216.

In our heat-to-heat variation studies, we concluded that room-temperature strength differences arise from differences in grain size and precipitate density.[6] The room-temperature yield strength and ultimate tensile strength of heat X6216 were about 55 MPa greater than for heat 36202. Since heats X6216 and 36202 differed little in grain size (Table 2), the room-temperature strength differences must be due to differences in the Mo_2C precipitate distribution in the proeutectoid ferrite. The dynamic strain aging peak for heat X6216 was also about 55 MPa above that for heat 36202.[6] Hence, we can conclude that both unaged heats developed similar dynamic strain aging peaks for similar test conditions.

Interaction solid solution hardening occurs by the interaction of Mo-C atom pairs or clusters with dislocations.[11] Such atom groupings would be expected to be precursors to Mo_2C precipitation. Evidently, the nucleation and growth kinetics for Mo_2C formation in heat 36202 is

different than for the other three heats. This could occur for several reasons. Because of different commercial annealing conditions, less Mo_2C formed in heat 36202, leaving more molybdenum and carbon in solution (because of a faster cooling rate, perhaps). Another possibility is that the kinetics is different in different heats, although this seems less likely. In either case, sufficient molybdenum and carbon for significant interaction solid solution hardening remains present longer in heat 36202. During aging, atom clusters could form, leading to enhanced strengthening. Since this point requires a longer time to be reached in heat 36202, optimum strengthening due to Mo_2C would be expected to require longer aging, as has been observed.

Metallography generally supports the observations on the precipitates. The proeutectoid ferrite of heat X6216 appeared to have the highest precipitate density before aging. After 20,000 hr the precipitate density for heat 36202 was probably greater than for heat X6216. Undoubtedly, heats 72768 and 72871 had the lowest densities of larger precipitates throughout the aging process. We previously discussed how different precipitation nucleation processes must give rise to the different precipitate morphology in various heats.[6]

The same effects noted for the tensile properties explain our results for creep, although here, data for only heats 72768 and X6216 were obtained. Nonclassical curves were obtained for both heats tested at 566°C, although they persisted to longer aging times for heat X6216. As discussed above, the nonclassical curves contain two steady-state stages; the first is due to interaction solid solution hardening. Thus, even though heats 72768 and X6216 did not show strength peaks due to interaction solid solution hardening, the effect persists to several thousand hours, even in these heats.

In the above discussion, the only dispersion-strengthening effect discussed was that due to Mo_2C. Maximum dispersion-strengthening effects by Mo_2C, which give rise to the peaks in the strength-aging time curves (Figs. 8–11), will occur for some optimum precipitate morphology. Over-aging is the result of particle coarsening (Ostwald ripening) and the replacement of Mo_2C by eta-carbide. This latter process should be well

in progress for most of the heats after 20,000 hr at 566°C. However, at lower temperatures, longer aging periods will be required to complete the process. Once this process is complete, further decreases in strength can be expected. For a 2 1/4 Cr-1 Mo steel aged 26,500 hr at 566°C in which only $M_{23}C_6$ and eta-carbides were present, yield strength and ultimate tensile strength at 566°C dropped to 138 and 193 MPa, respectively.[9]

SUMMARY AND CONCLUSIONS

Four commercial tubing heats of 2 1/4 Cr-1 Mo steel were aged at 454, 510, and 566°C for 1000, 2500, 5000, 10,000, and 20,000 hr. Room-temperature tensile tests were made on specimens from all heats aged under each condition. Tensile tests were also made at the aging temperature (i.e., specimens aged at 454°C were tested at 454°C, etc). For two heats, creep tests were made at 138 MPa at 566°C on specimens aged at all three temperatures, and a limited number of specimens aged at 454 and 510°C were tested at these same temperatures. The following observations and conclusions were made:

1. Room-temperature tensile properties varied with aging time and temperature. Minor changes occurred in the room-temperature ultimate tensile strengths, even after these specimens were aged for 20,000 hr at 566°C. More substantial changes occurred in yield strength. Although mainly strength decreases were noted after 20,000 hr, two heats showed increased strengths at room temperature.

2. When the tensile tests were made at aging temperatures, property changes after 20,000 hr were greater than at room temperature, and the greatest relative change occurred in ultimate tensile strength. Again, not all changes involved strength decreases; one heat showed strength increases at 454 and 510°C.

3. Relative strength decreases after 20,000 hr were greatest after aging at 566°C. The maximum decrease was between 30–40%, and the amount varied from heat to heat.

4. Property changes were not continuous to 20,000 hr. When strength was plotted against time, relative maxima and minima occurred.

5. We concluded that strength was determined by precipitation processes in the proeutectoid ferrite, which makes up the bulk of the microstructure. Early in the aging process, interaction solid solution hardening due to molybdenum and carbon in solid solution determines the strength. Later, dispersion-strengthening due to Mo_2C precipitates is the dominant strengthening mechanism. An optimum Mo_2C particle size and density leads to a strength peak, after which strength decreases. Eventually, Mo_2C is replaced by large globular eta-carbide particles with a further decrease in strength.

ACKNOWLEDGMENTS

Thanks are due the following people who helped the author complete this work: J. L. Griffith and L. T. Ratcliff, who performed the experimental work; C. W. Houck, who did the metallography; J. P. Hammond, A. E. Moorhead, C. R. Brinkman, and G. M. Slaughter, who reviewed the manuscript, R. R. Ihrig, who edited the manuscript; and Julia Bishop, who typed it.

REFERENCES

1. R. G. Baker and J. Nutting, "The Tempering of 2 1/4 Cr-1 Mo Steel After Quenching and Normalizing," *J. Iron Steel Inst. London* 192: 257–68 (1959).
2. K. F. Hale, "Study of Creep in a Chromium-Molybdenum Steel," *Proc. 4th Intern. Conf. Electron Microscopy*, vol. 1, pp. 650–58, Springer-Verlag, Berlin, 1960.
3. M. C. Murphy and G. D. Branch, "Metallurgical Changes in 2.25 CrMo Steels During Creep-Rupture Test," *J. Iron Steel Inst. London* 209: 546-61 (1971).
4. E. B. Norris, G. J. Schnabel, and R. D. Wylie, "Properties of Cr-Mo Piping Materials After Service at 1000 and 1050°F," paper presented at International Conference on Creep and Fatigue in Elevated-Temperature Applications, Philadelphia, 1973, and Sheffield, U.K., April 1974.

5. R. L. Klueh, *Creep-Rupture Properties of Decarburized and Aged 2 1/4 Cr-1 Mo Steel,* ORNL-5292 (August 1977).
6. R. L. Klueh, "Heat-to-Heat Variation of Tensile Properties of Annealed 2 1/4 Cr-1 Mo Steel," Proceedings of Symposium on Effects of Melting and Processing Variables on the Mechanical Properties of Steels, to be published.
7. R. L. Klueh, *Creep and Rupture Behavior of Annealed 2 1/4 Cr-1 Mo Steel,* ORNL-5219 (December 1976).
8. J. M. Leitnaker, R. L. Klueh, and W. R. Laing, "The Composition of Eta-Carbide Phase in 2 1/4 Cr-1 Mo Steel," *Metall. Trans.* 6A: 1949–55 (1975).
9. R. L. Klueh and J. M. Leitnaker, "An Analysis of the Decarburization and Aging Processes in 2 1/4 Cr-1 Mo Steel," *Metall. Trans.* 6A: 2089–93 (1975).
10. K. J. Irvine, J. D. Murray, and F. B. Pickering, "Structural Aspects of Creep-Resisting Steel," pp. 246–75 in *Structural Processes in Creep,* Iron and Steel Institute, London, 1961.
11. J. D. Baird and A. Jamieson, "High-Temperature Tensile Properties of Some Synthesized Iron Alloys Containing Molybdenum and Chromium," *J. Iron Steel Inst. London* 210: 841–46 (1972).
12. J. D. Baird and A. Jamieson, "Creep Strength of Some Synthesized Iron Alloys Containing Manganese, Molybdenum, and Chromium," *J. Iron Steel Inst. London* 210: 847–56 (1972).
13. R. L. Klueh, "Heat Treatment Effects on the Tensile Properties of Annealed 2 1/4 Cr-1 Mo Steel" accepted for publication in the *Journal of Nuclear Materials.*